

# Performance Study of A Deep Space Communications System with Low-Density Parity-Check Coding under Solar Scintillation

Qi Li, Liuguo Yin, Jianhua Lu

**Abstract**—The communication link is the only way for space probe to receive telecommand data from and return telemetry information to the control center on the earth. The design of deep space communication system has lots of challenging problems. For example, the solar scintillation effects can be significant for deep-space telecommunication links during superior solar conjunction. In this paper, the design and application of low-density parity-check (LDPC) coding scheme for deep space communication under solar scintillation condition is studied. In particular, the deep space communication channel under solar scintillation condition is modeled as a kind of Rician Channel that characterized by scintillation index, and the LDPC codes are optimized under such kind of channel mode to improve the bit-error rate (BER) performance. Simulation results reveal that compared with the convolutional codes the proposed LDPC codes could obtain 2.4 db and 2.5 db coding gain at 8.4 GHz (X-band) and 32 GHz (Ka-band), respectively. Moreover, simulation results also show that the deep space communication system with LDPC codes is much less sensitive to scintillation fading than that with convolutional codes.

**Keywords**—BP algorithm, channel capacity, LDPC codes, Rician channel, solar scintillation

## I. INTRODUCTION

DEEP space exploration is the way for human to know about the origins and evolution of the Earth, planets, solar system and the universe, which could thereby promote the development and cross-penetration innovation of planetary science, earth and planetary sciences, solar system evolution, space astronomy, space physics, space materials science, environmental science, microgravity space and other basic science disciplines. Deep space exploration is also the way for a better understanding of the life formation and evolution in the universe, and the way for us to enter into the universe to find new homelands.

During the human exploration of space, the communications link is the only way that enabling telecommands to be transmitted from the earth and telemetry information as well as scientific data to be returned from the probe, which may

Manuscript received August 3, 2011; Revised version received September 18, 2011. This work was supported in part by National Natural Science Foundation of China (No. 61021001, 61101072) and Program for New Century Excellent Talents in University (NCET).

Qi Li is with the Department of Electronic Engineering, Tsinghua University, Haidian District, Beijing, 100084, China (e-mail: qi-li09@mails.tsinghua.edu.cn).

Liuguo Yin is with the School of Aerospace, Tsinghua University, Haidian District, Beijing, 100084, China (e-mail: yinlg@tsinghua.edu.cn).

Jianhua Lu is with the Department of Electronic Engineering, Tsinghua University, Haidian District, Beijing, 100084, China (e-mail: lujh@wmc.ee.tsinghua.edu.cn)

directly dictates the success or failure of the space exploration mission.

The communication link in deep space environment faces many severe challenges. The first of which is the ultra-long communication distance. For geosynchronous satellite, the data communication distance is about 36,000 km. While for the data communication between the Mars probe and the control center on the earth, the data transmission distance may reach up to 384,000,000 km. Since the intensity of electromagnetic radiation decreases according to  $1/r^2$ , signals from deep space probes are usually very weak when they reach the Earth. In order to receive the faint signal back on Earth, large parabolic disc antennas are used to collect as much as possible of the faint signal. Meanwhile, since the electromagnetic radiation cannot move faster than the speed of light, considerable transmission delay is introduced in the communications, which making real time communications impossible, i.e., it takes over 5 hours for a signal from earth to reach the orbit of Pluto in the outer part of the solar system.

Moreover, the communication link between the earth and the space probe may encounter ionospheric scintillation during superior solar conjunction (see Fig. 1), when the Sun lies between the Earth and probe. The Earth-Probe distance is at or near maximum and the received signal is at its weakest level. In addition, the intervening charged particles of the solar corona in the signal path produce significant amplitude scintillation, phase scintillation, and spectral broadening effects, which increase as the Sun-Earth-Probe (SEP) angle ( $\theta$  in Fig. 1) decreases [1].

Several solutions could be used to deal with the situation, such as the implementation of channel coding, the increase of antenna aperture, and the reduction of project operations. While each of them has its limitations: First, the channel coding method in deep space communication at present is convolutional code, which has insufficient correcting ability in severe condition. Second, the increase of antenna aperture will greatly increase the construction cost as well as the operation complexity. Third, the reduction of project operations, such as invoking command moratoriums, downscaling tracking schedule and lowering data rates, will result in the unreliability of the whole system [2]-[4].

In this paper, we proposed to apply low-density parity-check (LDPC) codes instead of convolutional codes to the deep space communication system. Noted that for its near Shannon limit performance [5], [6], LDPC codes have been extensively applied in many communication and digital storage

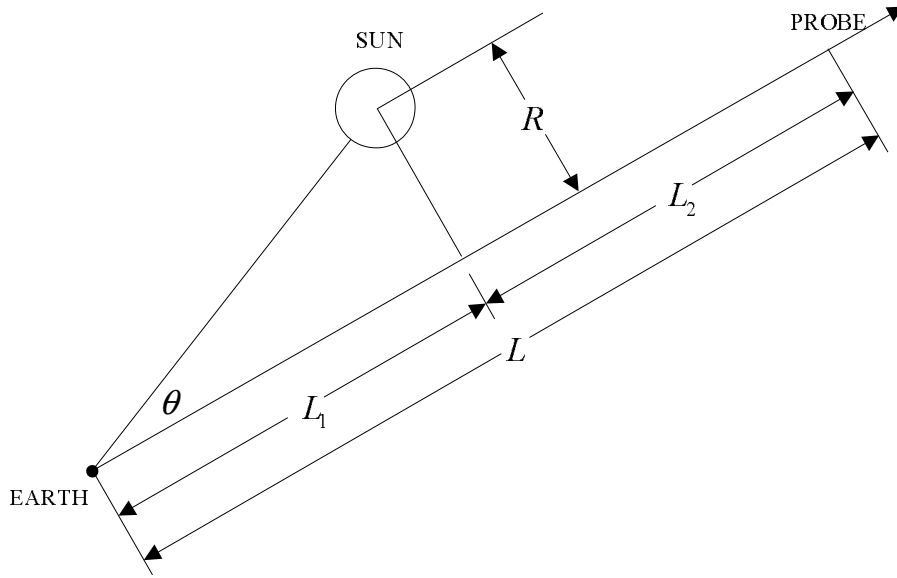


Fig. 1. Relevant solar conjunction geometry.

systems with high reliability requirements, and these years the applications have been expanded to aerospace field, such as Chang'e 2, the Chinese lunar probe launched in November 2010.

Since the deep space communication channel under solar scintillation condition is modeled as a kind of Rician Channel that characterized by scintillation index [7], we optimize the LDPC codes under such kind of channel mode to improve the BER performance. Simulation results reveal that compared with the convolutional codes the proposed LDPC codes could further obtain 2.4 db and 2.5 db coding gain at 8.4 GHz (X-band) and 32 GHz (Ka-band), respectively. Moreover, simulation results also show that the deep space communication system with LDPC codes is much less sensitive to scintillation fading than that with convolutional codes.

The rest of this paper is organized as follows. Section II addresses the scintillation modeling of the deep space communication channel under solar scintillation condition. Section III describes the optimization studies of the LDPC codes for application in deep space communications. Section IV presents the simulation and performance analysis of the LDPC codes over solar scintillation channels. Finally, conclusions are drawn in section V.

## II. CHANNEL MODEL UNDER SOLAR SCINTILLATION

A complex baseband model of scintillation communication system is depicted in Fig. 2. The received signal  $y(t)$  can be presented by

$$\begin{aligned} y(t) &= \alpha_{sc}(t) \cdot w(t) + n(t) \\ &= \alpha_{sc}(t) \cdot s(t)e^{j\theta(t)} + n(t) \end{aligned} \quad (1)$$

Where  $s(t)$  is the transmitted signal,  $\theta(t)$  is derived from channel estimation, and independent of the concerned signal

to noise ratio (SNR);  $\alpha_{sc}(t)$  is time-varying scintillation coefficient, produced by the solar scintillation;  $n(t)$  obeys Gaussian random distribution with zero mean and variance  $\sigma^2$  [8].

### A. Rician Statistical Model of Scintillation Channel

The scintillation coefficient  $\alpha_{sc}(t)$  is statistically modeled as a non-zero mean, complex Gaussian random process [8]-[12], i.e.,

$$\alpha_{sc}(t) = \sqrt{K_s} \cdot e^{j\phi} + n_{scint}(t) \quad (2)$$

where  $K_s$  is proportional to the signal power via the line-of-sight path (specular signal component);  $\phi$  is a constant phase shift randomly and uniformly distributed over the interval of  $[-\pi, \pi]$  and  $n_{scint}(t)$  is a (filtered) complex Gaussian process generated from scattered signal propagation over random paths (non line-of-sight) due to solar scintillation effects. The angular distribution of the random signal propagation paths is approximately Gaussian.

The signal fluctuation is measured by the scintillation index  $S_4$ :

$$S_4 = \sqrt{\frac{\text{var}\{|\alpha_{sc}(t)|^2\}}{\{E|\alpha_{sc}(t)|^2\}^2}} \quad (3)$$

The average signal power received via the scattered paths is proportional to:  $\sigma_{nsc}^2 \equiv E|n_{scint}(t)|^2$  and the total received signal power is presented by:  $S = (K_s + 2\sigma_{nsc}^2) \cdot P_s$ , where  $P_s \equiv E|w(t)|^2 = E\{s(t)^2\}$  is the transmitted signal power (see Fig. 2). Assume that the amplitude scintillation causes no loss in the long-term average received signal power. Then the specular and scattered signal power components must meet the constraint  $K_s + 2\sigma_{nsc}^2 = 1$ .

The envelop of the scintillation coefficient  $R_{sc} = |\alpha_{sc}(t)|$  has a character of Rician distribution, i.e.,

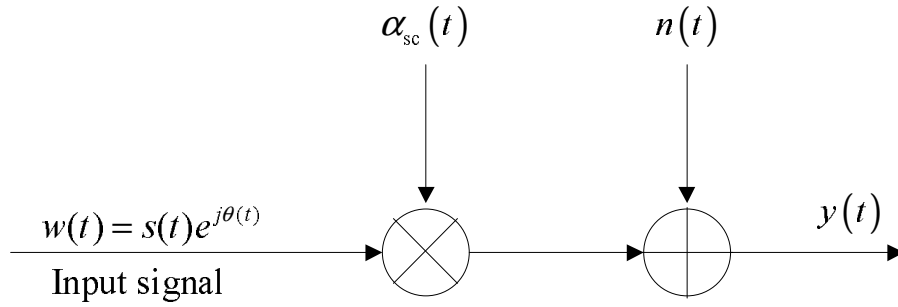


Fig. 2. Complex baseband channel simulation model.

$$p_{rsc}(R) = \frac{R}{\sigma_{nsc}^2} \cdot e^{-\gamma} \cdot e^{-\frac{R^2}{2\sigma_{nsc}^2}} \cdot I_0\left\{R\sqrt{\frac{2\gamma}{\sigma_{nsc}^2}}\right\}, R \geq 0 \quad (4)$$

where  $\gamma \equiv K_s/2\sigma_{nsc}^2$  is the Rician factor, defined as the ratio of received specular power to random power, and  $I_0\{x\}$  is the zeroth-order, modified Bessel function of the first kind. The relationship of scintillation index  $S_4$  and the Rician factor  $\gamma$  can be expressed as [13]

$$\gamma = \frac{(1 - S_4^2)^{1/2}}{1 - (1 - S_4^2)^{1/2}} \quad (5)$$

Then the parameters  $K_s$  and  $\sigma_{nsc}^2$  are related to the scintillation index  $S_4$  by

$$K_s = (1 - S_4^2)^{1/2} \quad (6)$$

$$\sigma_{nsc}^2 = \frac{1 - (1 - S_4^2)^{1/2}}{2} \quad (7)$$

Notice that  $S_4$  is between 0 and 1. When  $S_4 \rightarrow 0$ , it translates to an ideal non-fading channel, with  $0 < S_4 < 1$ , it is Rician fading, and in the limit  $S_4 \rightarrow 1$  (no line-of-sight received path), it reduces to the Rayleigh fading.

#### B. The Shannon Limit with Different Scintillation Index

For binary phase shift keying (BPSK) modulation,  $s \in \{-\sqrt{E_s}, \sqrt{E_s}\}$  maps the code symbol  $x \in \{1, 0\}$ , while  $E_s$  is the symbol energy. Assume the Rician fading factor  $\alpha_{sc}$  is given. Then the conditional probability density function of the matched filter output is [14]

$$p(y|s, \alpha_{sc}) = \frac{1}{\sqrt{2\pi\sigma^2}} e^{-\frac{(y-s\alpha_{sc})^2}{2\sigma^2}} \quad (8)$$

The capacity of the channel is defined by [15]

$$\begin{aligned} C &= \max_{p_s(s)} \{I(S; Y|A_{SC})\} \\ &= \max_{p_s(s)} \left\{ E_{p(s, y, \alpha_{sc})} \left\{ \log \frac{p(y|s, \alpha_{sc})}{\sum_z p_s(z) \cdot p(y|z, \alpha_{sc})} \right\} \right\} \end{aligned} \quad (9)$$

where  $E_p(x)$  is the mathematical expectation of variable  $x$  with probability distribution of  $p$ . The probability density function  $p(s, y, \alpha_{sc})$  can be written as (10) due to the independency between  $s$  and  $\alpha_{sc}$ .

$$p(s, y, \alpha_{sc}) = p(y|s, \alpha_{sc}) \cdot p(s) \cdot p(\alpha_{sc}) \quad (10)$$

If  $p(s)$  satisfies the equal-probability distribution, the  $I(S; Y|A_{SC})$  reaches the maximum.

$$\begin{aligned} C &= \frac{1}{2} \sum_{s=\pm\sqrt{E_s}} \int_0^\infty \int_{-\infty}^\infty p(\alpha_{sc}) \cdot p(y|s, \alpha_{sc}) \\ &\quad \cdot \log_2 \left( \frac{p(y|s, \alpha_{sc})}{\frac{1}{2} \sum_{z=\pm\sqrt{E_s}} p(y|z, \alpha_{sc})} \right) \cdot dy \cdot d\alpha_{sc} \\ &= \int_0^\infty \int_{-\infty}^\infty p(\alpha_{sc}) \cdot p(y|s = \sqrt{E_s}, \alpha_{sc}) \\ &\quad \cdot \log_2 \left( \frac{2p(y|z = \sqrt{E_s}, \alpha_{sc})}{p(y|z = \sqrt{E_s}, \alpha_{sc}) + p(y|z = -\sqrt{E_s}, \alpha_{sc})} \right) \\ &\quad \cdot dy \cdot d\alpha_{sc} \\ &= 1 - \int_0^\infty \int_{-\infty}^\infty p(\alpha_{sc}) \cdot p(y|s = \sqrt{E_s}, \alpha_{sc}) \\ &\quad \cdot \log_2 \left( 1 + \frac{p(y|z = -\sqrt{E_s}, \alpha_{sc})}{p(y|z = \sqrt{E_s}, \alpha_{sc})} \right) \cdot dy \cdot d\alpha_{sc} \end{aligned} \quad (11)$$

From (8), we can get

$$\frac{p(y|z = -\sqrt{E_s}, \alpha_{sc})}{p(y|z = \sqrt{E_s}, \alpha_{sc})} = -2y\alpha_{sc}\sqrt{E_s}/\sigma^2 \quad (12)$$

Then the capacity  $C$  can be written as .

$$\begin{aligned} C &= 1 - \int_0^\infty \int_{-\infty}^\infty p(\alpha_{sc}) \cdot p(y|s = \sqrt{E_s}, \alpha_{sc}) \\ &\quad \cdot \log_2(1 + e^{-2y\alpha_{sc}\sqrt{E_s}/\sigma^2}) \cdot dy \cdot d\alpha_{sc} \end{aligned} \quad (13)$$

The double integral function is written as (14) through (4) and (8)

$$\begin{aligned} f(y, \alpha_{sc}) &= p(\alpha_{sc}) \cdot p(y|s = \sqrt{E_s}, \alpha_{sc}) \\ &\quad \cdot \log_2(1 + e^{-2y\alpha_{sc}\sqrt{E_s}/\sigma^2}) \\ &= \frac{\alpha_{sc}}{\sigma_{nsc}^2} \cdot e^{-\gamma} \cdot e^{-\frac{\alpha_{sc}^2}{2\sigma_{nsc}^2}} \cdot I_0\left\{\alpha_{sc}\sqrt{\frac{2\gamma}{\sigma_{nsc}^2}}\right\} \\ &\quad \cdot \frac{1}{\sqrt{2\pi\sigma^2}} e^{-\frac{(y-\alpha_{sc}\sqrt{E_s})^2}{2\sigma^2}} \\ &\quad \cdot \log_2(1 + e^{-2y\alpha_{sc}\sqrt{E_s}/\sigma^2}) \end{aligned} \quad (14)$$

Put  $\sigma^2 = 1/2$ , (14) can be written as

$$\begin{aligned} f(y, \alpha_{sc}) &= \frac{\alpha_{sc}}{\sigma_{nsc}^2} \cdot e^{-\gamma} \cdot e^{-\frac{\alpha_{sc}^2}{2\sigma_{nsc}^2}} \cdot I_0\left\{\alpha_{sc}\sqrt{\frac{2\gamma}{\sigma_{nsc}^2}}\right\} \\ &\quad \cdot \frac{1}{\sqrt{\pi}} e^{-(y-\alpha_{sc}\sqrt{E_s})^2} \cdot \log_2(1 + e^{-4y\alpha_{sc}\sqrt{E_s}}) \end{aligned} \quad (15)$$

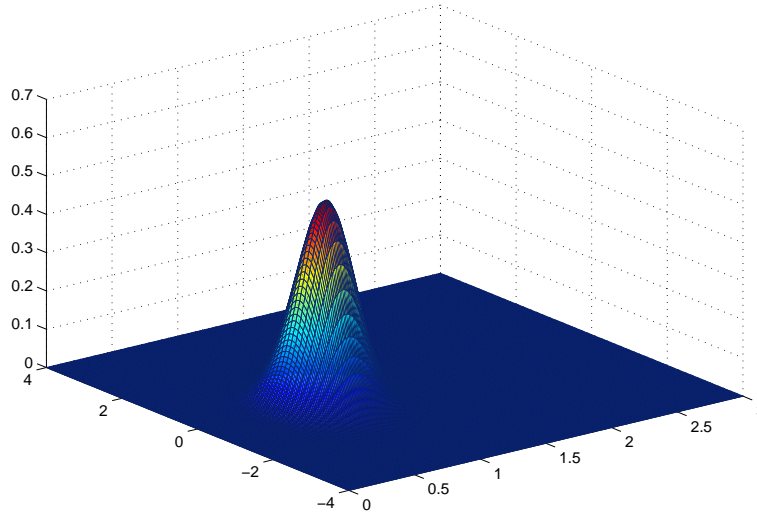


Fig. 3. The double integral function with  $S_4 = 0.37$  and  $\sqrt{E_s} = 1$ .

TABLE I  
THE SHANNON LIMIT WITH DIFFERENT CODE RATES  $R$  AND SCINTILLATION INDEX  $S_4(E_b/N_0$  dB)

$R \backslash S_4$	0.10	0.20	0.30	0.60	0.90	1.00
0.01	-1.5748	-1.5613	-1.5529	-1.5469	-1.5341	-1.529
0.30	-0.6115	-0.5804	-0.5353	-0.2961	0.1058	0.2565
0.50	0.2025	0.2521	0.3309	0.7852	1.5676	1.8309
0.80	2.0796	2.1746	2.3704	3.4699	5.41	5.9437
0.99	6.0339	6.3350	6.877	11.6661	17.8327	19.006

$\gamma$  and  $\sigma_{nsc}$  relate to the scintillation index  $S_4$  through (5) and (7). When  $S_4 = 0.37$  and  $\sqrt{E_s} = 1$ ,  $f(y, \alpha_{sc})$  is shown in Fig. 3.

In most area, the function  $f(y, \alpha_{sc})$  tends to be 0 and only a small area has contribution to the volume of the figure, so the generalized double integral can be calculated into the numerical calculation of double definite integral.

According to Shannon's second theorem, if the information transmission rate  $R$  is not larger than the channel capacity  $C$ , there exists a coding system such that the information bit can be transmitted over the channel with an arbitrary small frequency of errors. Let  $R = C$ , finally the shannon limit is given by

$$\begin{aligned} \left\{ \frac{E_b}{N_0} \right\}_{R=C} &= \frac{1}{R} \cdot \left\{ \frac{E_s}{N_0} \right\}_{R=C} \\ &= \frac{1}{R} \cdot \left\{ \frac{E_s}{2\sigma^2} \right\}_{R=C} = \frac{E_s}{R} \end{aligned} \quad (16)$$

When  $E_s$  takes different values, the Shannon limit with different code rate  $R$  and different scintillation index  $S_4$  can be calculated (see Table I).

### III. THE OPTIMIZATION STUDIES OF LDPC CODES OVER RICIAN CHANNEL

As originally suggested by Tanner [16], LDPC codes can be well represented by bipartite graphs, which consist of variable nodes, check nodes and the edges emanating from these nodes.

Variable nodes correspond to the elements of a codeword, while check nodes correspond to the set of parity-check constraints which define the code. The degree distribution of variable (check) nodes determine the number of nonzero elements in the row (column) of check parity matrix of LDPC codes, and a polynomial is used to represent the degree distribution. A degree distribution pair  $(\lambda, \rho)$  is defined as [17]

$$\lambda(x) = \sum_{i=1}^{d_v} \lambda_i x^{i-1} \quad (17)$$

$$\rho(x) = \sum_{i=1}^{d_c} \rho_i x^{i-1} \quad (18)$$

where  $\lambda_i$  ( $\rho_i$ ) represents the fraction of edges emanating from variable (check) nodes of degree  $i$ , and the  $d_v$  ( $d_c$ ) denotes the maximum variable (check) degree.

The method used to optimize degree distributions is Gaussian approximation and the decoding of LDPC codes is based on belief-propagation (BP) algorithm. Under the BP algorithm, and message passing in general, variable nodes and check nodes exchange messages iteratively.

The log-likelihood ratios (LLRs) are used as messages, i.e.,

$$v = \log \frac{p(y|x=1)}{p(y|x=-1)} \quad (19)$$

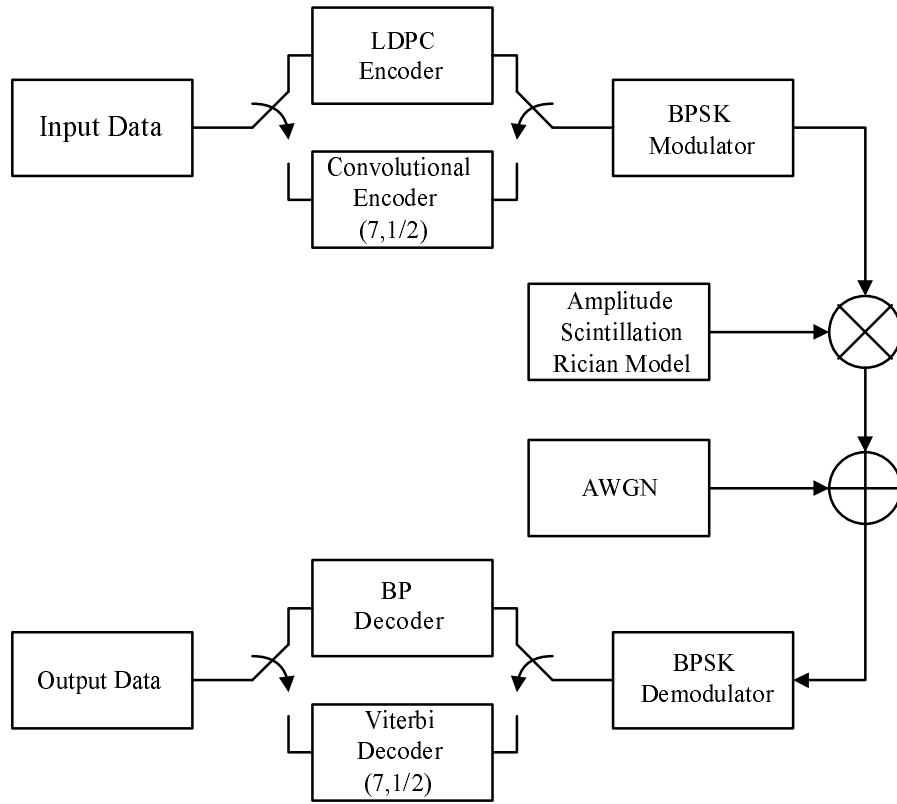


Fig. 4. Channel simulation model.

TABLE II  
THE VALUE TABLE OF  $\lambda_i$  AND  $\rho_i$  (N=2032)

$\lambda_1$	$\lambda_2$	$\lambda_3$	$\lambda_6$	$\rho_6$	$\rho_7$
0.001126	0.283784	0.214527	0.500563	0.006757	0.993243

as the output message of a variable node, where  $x$  is the bit value of the node and  $y$  denotes all the information available to the node up to the present iteration obtained from edges other than the one carrying  $v$ . Likewise, the output of a check node is defined as

$$u = \log \frac{p(y'|x' = 1)}{p(y'|x' = -1)} \quad (20)$$

Let  $v$  be a message from a variable node to a check node. Under sum-product decoding,  $v$  is equal to the sum of all incoming LLRs. It is expressed as (21), and  $i$  is the degree of the variable node.

$$v = \sum_{a=0}^{i-1} u_a \quad (21)$$

where  $u_a$  ( $a = 1, 2, \dots, i-1$ ) are the incoming LLRs from the neighbors of the variable node except the check node that gets the message  $v$ , and  $u_0$  is the observed LLR of the output bit associated with the variable node.

In Gaussian approximation, assume  $u \sim N(m_u, 2m_u)$ ,  $v \sim N(m_v, 2m_v)$ , then at the  $l$ -th iteration, the mean of the output of a variable node with degree  $i$  is defined as:

$$m_{v,i}^{(l)} = m_{u_0} + (i-1) \cdot m_u^{(l-1)} \quad (22)$$

where  $u_0$  is LLR message of the received signal after the channel soft demodulation, when all 1 codes are transmitted, then in AWGN channel, with noise variance  $\sigma^2$ ,  $u_0 \sim N(\frac{2}{\sigma^2}, \frac{4}{\sigma^2})$ .

The decoding of the check node with degree  $j$  is given as:

$$\tanh\left(\frac{u}{2}\right) = \prod_{t=1}^{j-1} \tanh\left(\frac{v_t}{2}\right) \quad (23)$$

According to the assumption that the LLR messages have Gaussian distribution, the probability density function of the soft decoding output at the  $l$ -th iteration is given as (24) by calculation.

$$f_d^{(l)}(x) = \frac{1}{\sqrt{4\pi \cdot (m_{u_0} + \sum_{i=1}^{d_v} \lambda_i \cdot i \cdot m_u^{(l)})}} \cdot \exp\left\{-\frac{(x - m_{u_0} - \sum_{i=1}^{d_v} \lambda_i \cdot i \cdot m_u^{(l)})^2}{4 \cdot (m_{u_0} + \sum_{i=1}^{d_v} \lambda_i \cdot i \cdot m_u^{(l)})}\right\} \quad (24)$$

According to (24), finally the output error-bit probability of decoding after the  $l$ -th iteration is given as

$$p_e^{(l)} = \int_{-\infty}^0 f_d^{(l)}(x) dx \quad (25)$$

(25) is used to analyze the change of the output error-bit probability of decoding with the iteration number, and

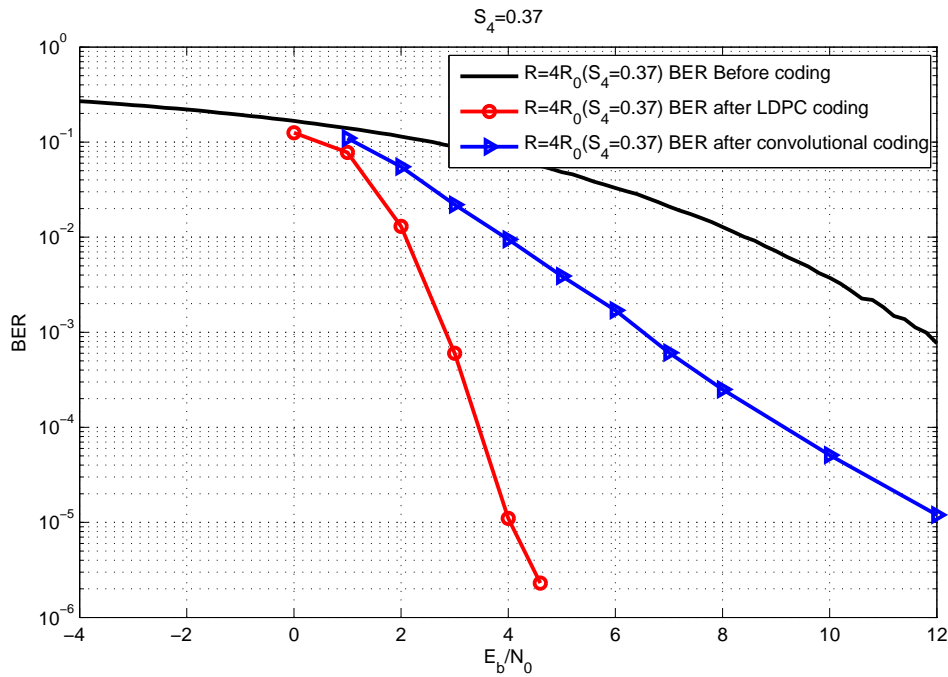


Fig. 5. Telecommunication link performance at X-band with  $R = 4R_0$ .

the impact of the degree distribution pair on the decoding performance.

Besides, according to BP algorithm, if the received signals at the channel output satisfy the symmetry condition and stability condition, the probabilities of the decoding error can be arbitrary small, otherwise it must larger than a certain value. Rician channel has been proved to satisfy the symmetry condition, and the stability condition is described as [18]

$$\lambda'(0) \cdot \rho'(1) < e^s = \frac{1 + 2 \cdot (1 + \gamma) \cdot \sigma_{\text{rician}}^2}{2 \cdot (1 + \gamma) \cdot \sigma_{\text{rician}}^2} \cdot e^{\frac{\gamma}{1 + 2 \cdot (1 + \gamma) \cdot \sigma_{\text{rician}}^2}} \quad (26)$$

According to (5) and (7), (26) can be written as

$$\lambda'(0) \cdot \rho'(1) < 2 \cdot e^{\frac{(1 - S_4^2)^{1/2}}{2 \cdot [1 - (1 - S_4^2)^{1/2}]}} \quad (27)$$

Based on (25) and (27), the degree distribution parameters  $\lambda_i$  ( $\rho_i$ ) can be optimized to make the LDPC codes transmitted through the Rician channel to get good performance.

#### IV. NUMERICAL SIMULATIONS AND ANALYSIS

The simulation is based on the link model as shown in Fig. 4, with the assumption of an ideal receiver, that is, the assumption of perfect carrier and subcarrier tracking as well as symbol synchronization. The degree distribution pairs  $(\lambda, \rho)$  after optimization using (25) and (27) are listed in Table II with code length  $n$  of 2032. In particular, the code rate  $r$  is 1/2, which is similar to the (7, 1/2) convolutional code that the Solar Probe mission has used [24]. The degradation caused by amplitude scintillation is simulated at both 8.4 GHz (X-band) and 32 GHz (Ka-band) for the case of BPSK modulation

with LDPC codes. The maximum iteration number is 50. For comparison, the (7, 1/2) convolutional codes are also simulated with Viterbi decoding. The effects due to scintillation are introduced through (6) and (7). The simulation BER performance at X-band is shown in Fig. 5, Fig. 6, Fig. 7 and Fig. 8.

In Fig. 5, the Sun-Probe distance ( $R$  in Fig. 1) is 4 solar radii ( $R_0$  in Fig. 1) and the corresponding scintillation index  $S_4$  is 0.37. The simulation shows that at  $BER = 10^{-5}$ , which is usual requirement for deep-space telecommunication link, the link performance of LDPC codes is much better than convolutional codes with coding gain about 8 dB.

The Sun-Probe distance  $R$  in Fig. 6 is 5 solar radii and the corresponding scintillation index  $S_4$  is 0.23, as the solar scintillation effects become smaller along with the increase of the Sun-Probe distance. At  $BER = 10^{-5}$ , the coding gain between LDPC codes and convolutional codes is about 3.3 dB.

In Fig. 7, the Sun-Probe distance  $R$  increases to 6 solar radii while the scintillation index  $S_4$  decreases to 0.162. At this Sun-Probe distance, the solar scintillation effects become smaller further. At  $BER = 10^{-5}$ , the link performance difference between LDPC codes and convolutional codes decreases to about 2.6 dB.

The Sun-Probe distance  $R$  in Fig. 8 increases to 8 solar radii. The distance is so far that the solar scintillation has slight impact on the communication link with the scintillation index  $S_4 = 0.099$ . The coding gain between LDPC codes and convolutional codes now becomes 2.4 dB.

From the figures, we can draw the conclusion that at  $BER = 10^{-5}$ , which can satisfy the deep-space telecommunication link requirement, the link performance of LDPC codes is better than convolutional codes with coding gain more than 2.4 dB at least,

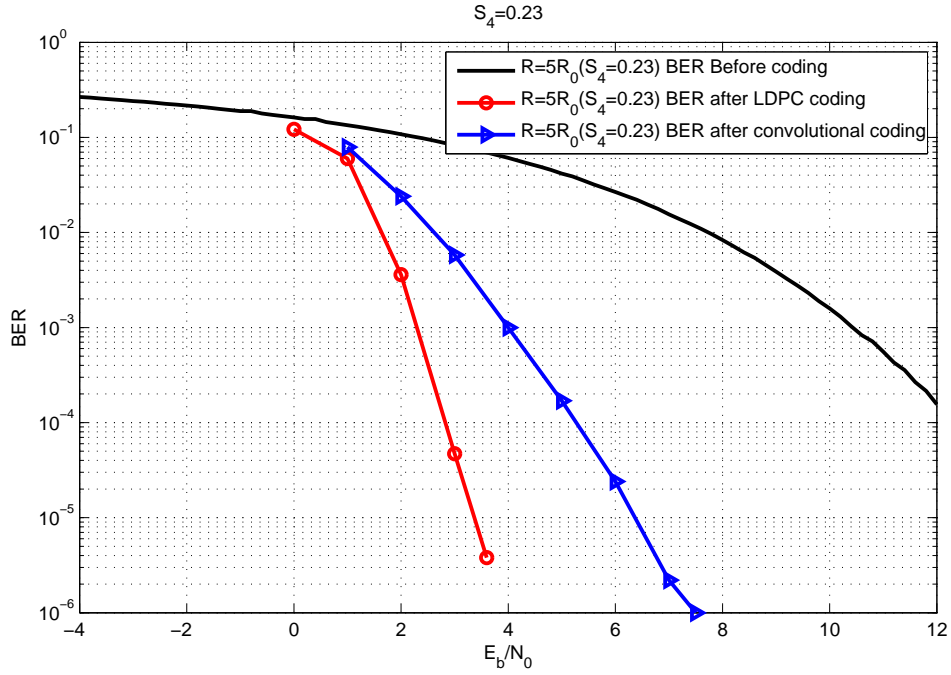


Fig. 6. Telecommunication link performance at X-band with  $R = 5R_0$ .

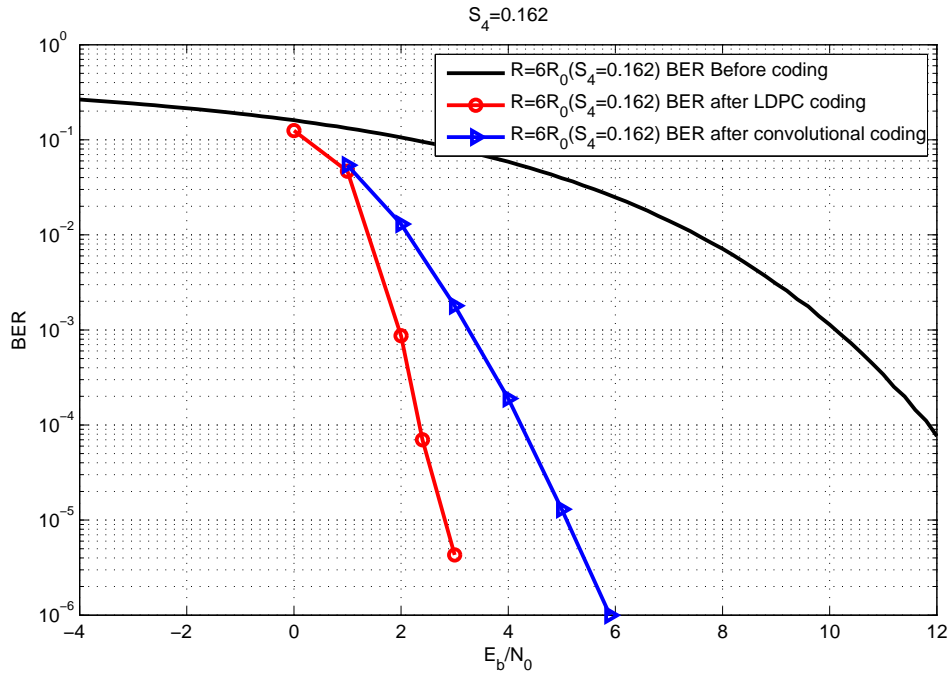


Fig. 7. Telecommunication link performance at X-band with  $R = 6R_0$ .

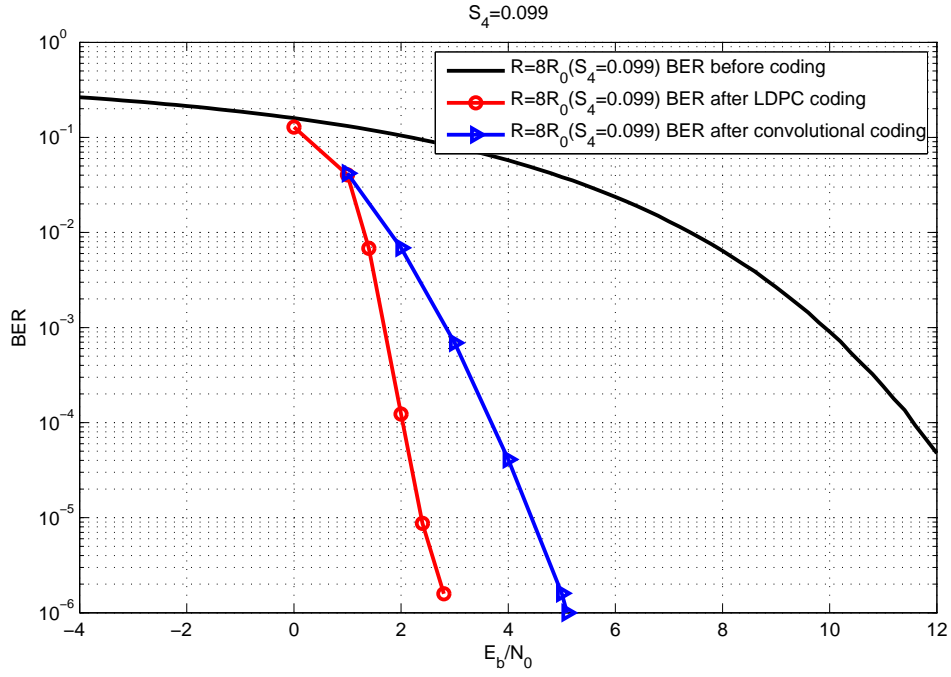


Fig. 8. Telecommunication link performance at X-band with  $R = 8R_0$ .

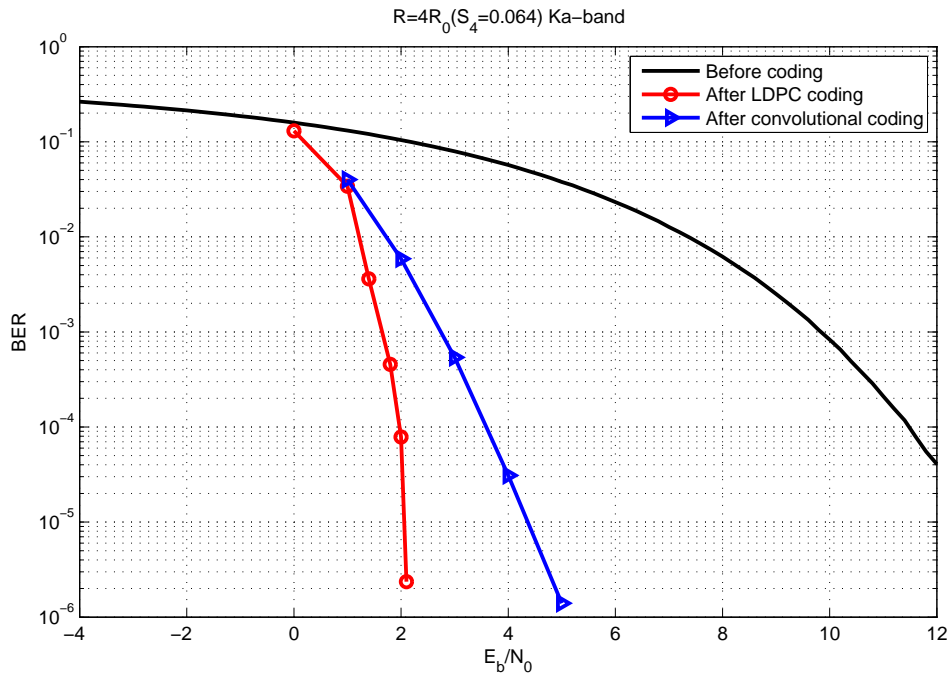


Fig. 9. Telecommunication link performance at Ka-band with  $R = 4R_0$ .

and with the increase of scintillation index  $S_4$ , the performance of convolutional codes degrades seriously, while LDPC codes represents an excellent performance of fading resistance. The difference of  $E_b/N_0$  of the figures and the Shannon limits in Table I is about 3 dB. The difference can be decreased by increasing the code length and the maximum iteration number.

Fig. 9 displays the link BER performance results at Ka-band, where the probe is assumed to be at perihelion with the Sun-Probe distance  $R = 4R_0$  and the scintillation index  $S_4 = 0.064$ , which is much smaller than X-band at the same Sun-Probe distance ( $S_4 = 0.37$ ) due to the high frequency. The link performance of LDPC codes is better than convolutional codes with coding gain about 2.5 db at  $BER = 10^{-5}$ .

## V. CONCLUSIONS

LDPC codes can give very good performance for communication under solar scintillation condition. In addition, their complexity can be reduced to the admissible level by using semi-random structure. Therefore, LDPC codes are very powerful and useful when they are applied to telemetry information transmissions in deep space communications.

## ACKNOWLEDGMENT

The authors would like to thank the anonymous reviewers for very insightful comments which greatly improved the quality of this manuscript.

## REFERENCES

- [1] E. J. Fremou and H. F. Bates, "Worldwide behavior of average VHF-UHF scintillation," *Radio Sci.*, vol. 6, pp. 863-869, Oct. 1971.
- [2] Robert S. Bokulic, William V. Moore, "The NEAR Solar Conjunction Experiment," JHU APPLIED PHYSICS LAB SER4340 NO.164.1998
- [3] D. Morabito, S. Shambayati, S. Butman, D. Fort, and S. Finley, "Communications with Mars During Periods of Solar Conjunction: Initial Study Results," *IPN Progress Report 42-147*, Nov.15,2001
- [4] D. Morabito, S. Shambayati, S. Butman, D. Fort, and S. Finley, "The 1998 Mars Global Surveyor Solar Corona Experiment," *The Telecommunications and Mission Operations Progress Report 42-142*, Apr.6 2000
- [5] R. G. Gallager, *Low-Density Parity Check Codes*. Cambridge, MA: MIT Press, 1963.
- [6] D. J. MacKay and R. M. Neal, "Near Shannon limit performance of low density parity check codes," *IEE Electronics Letters*, vol. 32, no. 18, pp. 1645- 1646, Aug. 1996.
- [7] Kullstam P. A. and Keskinen M. , "Ionospheric Scintillation Effects on UHF Satellite Communications," *MILCOM*, 2000.
- [8] Z. Ye and E. Satorius, "Channel Modeling and Simulation for Mobile User Objective System (MUOS)-Part I: Flat Scitillation and Fading," *ICC'03*, pp. 3503- 3510, Nov. 2003.
- [9] Nicholson J., Gerstein B., "The Department of Defense's Next Generation Narrowband Satellite Communications System, the Mobile User Objective System(MUOS)," *MILCOM* 2000.
- [10] Sapp, A., Jr., "Mobile User Objective System (MUOS): future satellite communications for the mobile warfighter," *MILCOM* 2000.
- [11] SPAWAR, "Mobile User Objective System (MUOS) Performance Specification (MPS) for Concept Exploration," November, 2000.
- [12] Kullstam P.A., "Communications Diversity Advantages for the Mobile User Objective System, *Milcom* 2000.
- [13] P. Shaft, "On the Relationship between Scintillation Index and Rician Fading," *IEEE Trans.*, Comm., pp.731-732, May 1974.
- [14] Xu Hua, Xu Cheng-qi and Xiaochuan Zheng, "Optimization of Irregular LDPC codes on Rician Channel," *Proc. Wireless Communications, Networking and Mobile Computing*, 2005.
- [15] Hong Wen, Chusheng Fu and Liang Zhou *Principle and Application of LDPC codes*. Chengdu, China: University of Electronic Science and Technology of China Press, May 2006.
- [16] M.Tanner, "A recursive approach to low complexity codes," *IEEE Trans. Inform. Theory*, vol. IT-27, pp.533-547, Sep. 1981.

- [17] T J Richardson, M A Shokrolahi , R L Urbanke, "Design of capacity-approaching irregular low Density parity check codes," *IEEE Trans. Inform. Theory*, pp.619- 637, Feb. 2001.
- [18] Lin Jiaru, Wu weiling, "Performance analysis of LDPC codes on Rice channel," *Journal of Beijing University of Posts and telecommunications*, vol. 27, no. 2, pp. 48-53, 2004.
- [19] Lin Jiaru and Wu Weiling, "Performance of Irregular LDPC codes on Rician-Rading Channel" *Acta Electronic Sinica*, vol. 33, no. 1, Jan. 2006.
- [20] Jin Sha, Minglun Gao, Zhongjin Zhang, Li Li, and Zhongfeng Wang, "Low complexity, memory efficient decoder architecture for quasi-cyclic LDPC codes," *WSEAS Transactions on Circuits and Systems*, 5(4): 590-5, Apr. 2006
- [21] Malema G and Liebelt M, "Deterministic methods for constructing structured LDPC codes with girth six and eight," *WSEAS Transactions on Computers*, 5(5): 1096-101, May 2006
- [22] Aiin C J and Fujise M, "Iterative decoding with LDPC based unitary matrix modulation with splitting over the coherence bandwidth for OFDM," *WSEAS Transactions on Computers*, 3(1): 230-5, Jan. 2004
- [23] Ontiveros B, Soto I and Carrasco R, "Construction of an elliptic curve over binary finite fields to concatenate with LDPC codes in wireless communication," *WSEAS Transactions on Communications*, 5(9): 1758-62, Sep. 2006
- [24] Y.Feria, M.Belongie, T.McPheeters and H.Tan, "Solar Scintillation Effects on Communication Links at Ka-band and X-band," *The Telecommunications and Data Acquisition Progress Report 42-129*, JPL Pasadena, California, May 15, 1997.
- [25] D. Morabito, "Solar Corona Amplitude Scintillation Modeling and Comparison to Measurements at X-Band and Ka-Band," *JPN Progress Report 42-153*, May 15 2003.

**Qi Li** was born in Hunan province, China, on October 16, 1984. She received the bachelor degree in electrical science and technology and master degree in information and communication engineering in the school of electronic and information engineering from Beijing University of Aeronautics and Astronautics (BUAA), Beijing, China in 2006 and 2009, respectively. She is currently working toward the Ph.D degree in the department of electronic engineering, Tsinghua University, Beijing, China. Her research interests include deep space communication systems and information theory.

**Liuguo Yin** was born in Guangxi Province, China, in 1977. He received the M.S. and Ph.D. degrees from Tsinghua University, Beijing, China, in 2002 and 2005, respectively.

From March 2005 to March 2007, he was a research assistant with the School of Aerospace, Tsinghua University. From April 2007 to March 2008, he was an ERCIM postdoctoral fellow with the Norwegian University of Science and Technology (NTNU), Trondheim, Norway. Since April 2008, he came back to Tsinghua University and worked as a research assistant. In 2009, he was promoted to Associate Professor. His current research interests include channel coding, joint source-channel coding, wireless sensor network, wireless channel estimation, MIMO-OFDM systems, and wireless multimedia communication systems.

Dr. Yin is a member of IEEE communication society.

**Jianhua Lu** was born in Jiangsu province, China, on July 14, 1963. He received the bachelor degree and master degree in the department of electronic engineering, Tsinghua University, Beijing, China in 1986 and 1989, respectively, and Ph.D in Electronic & Electronic Engineering from the Hong Kong University of Science & Technology.

He is a professor in the department of electronic engineering, Tsinghua University, Beijing, China. His research interests include wireless communication systems, wireless multimedia communications, image communications and wireless networking.

Prof. Lu is a senior member of IEEE Communication Society and Signal Processing Society.